ELSEVIER

Journal of Fluids and Structures 26 (2010) 517–525

JOURNAL OF FLUIDS AND STRUCTURES

www.elsevier.com/locate/jfs

Special Brief Communication

Dynamics of a cantilevered pipe discharging fluid, fitted with a stabilizing end-piece

S. Rinaldi, M.P. Païdoussis*

Department of Mechanical Engineering, McGill University, 817 Sherbrooke Street West, Montreal, QC, Canada H3A 2K6

Received 24 March 2009; accepted 8 January 2010
Available online 1 April 2010

Abstract

In this communication, the dynamics of a flexible cantilevered pipe fitted with a special end-piece is considered, both theoretically and experimentally. This end-piece can be configured in two ways: (i) with the flow going straight through, unimpeded, and emerging at the free end as a jet, and (ii) with the straight-through path blocked, so that the flow is discharged radially from a number of holes perpendicular to the pipe. The dynamics in the first case is similar to that of a pipe with no end-piece: the system loses stability by flutter via a Hopf bifurcation, though the dynamics becomes more complex at higher flow velocities. The dynamics in the second case is entirely different: the system remains stable over the full range of flow velocities considered. This study provides insight into the mechanism of flutter of cantilevered pipes conveying fluid and the key role played by the mathematically obvious but physically counter-intuitive compressive follower force generated by the straight-through discharging jet.

Keywords: Cantilevered pipe; Experiments; Fluid–structure interactions; Flutter; Stabilizing mechanism

1. Background information

It is known, both theoretically and experimentally, that a cantilevered pipe conveying fluid is a nonconservative system: at low flow velocities it is subject to flow-induced damping, and at a sufficiently high flow velocity it loses stability by flutter via a Hopf bifurcation. Considering for the present a ''plain pipe'', with no end-piece at the free end, the simplest linear form of the equation of motion is (Païdoussis, 1998)

$$EI\frac{\partial^4 w}{\partial x^4}+MU^2\frac{\partial^2 w}{\partial x^2}+2MU\frac{\partial^2 w}{\partial x\partial t}+(M+m)\frac{\partial^2 w}{\partial t^2}=0, \tag{1}$$

where EI is the flexural rigidity, w the lateral deflection of the pipe, x the axial coordinate, M the mass of the fluid per unit length, U the dimensional flow velocity, m the mass of the pipe per unit length, and t is time. The dynamics may be elucidated by considering the work done by the fluid-dynamic forces on the pipe over a period of oscillation T, which

*Corresponding author. Fax: +1 514 398 7365.
E-mail address: mary.fiorilli@mcgill.ca (M.P. Païdoussis).

0889-9746/$ - see front matter © 2010 Elsevier Ltd. All rights reserved.
doi:10.1016/j.jfluidstructs.2010.01.004

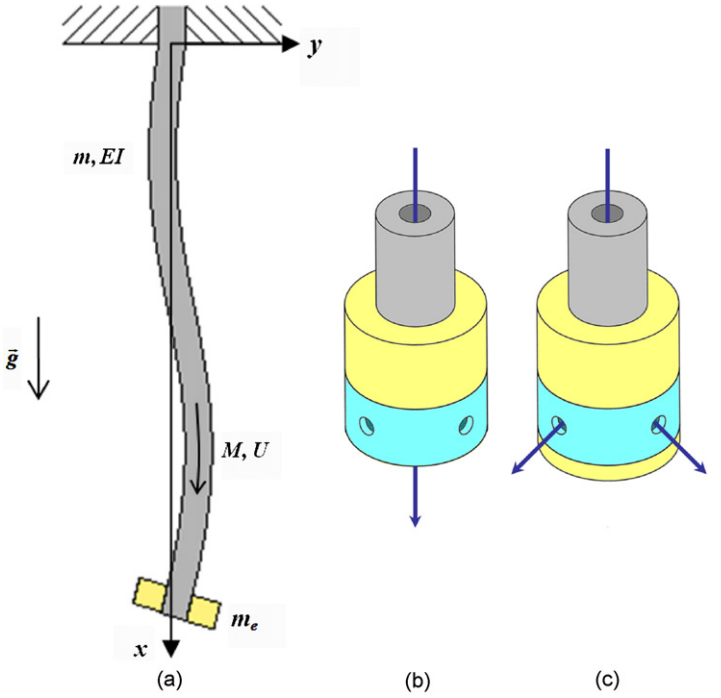

Fig. 1. (a) The flexible cantilevered pipe fitted with the special end-piece, (b) the unplugged end-piece in the straight-through flow configuration and (c) the plugged end-piece in the 90° diverted-flow configuration.

from Eq. (1) is found to be (Païdoussis, 1998)

$$\Delta W = -MU\int_0^T \left[\left(\frac{\partial w}{\partial t}\right)_L^2 + U\left(\frac{\partial w}{\partial t}\right)_L\left(\frac{\partial w}{\partial x}\right)_L\right] \mathrm{d}t \neq 0, \tag{2}$$

where the subscript L denotes a quantity evaluated at $x = L$. For sufficiently small values of U, it is clear that the first term in Eq. (2) is dominant, and ΔW is negative. Therefore, the cantilevered pipe remains stable because free motions of the system are damped. However, for sufficiently large values of U, it is evident from Eq. (2) that ΔW can be positive if the free-end slope, $(\partial w/\partial x)_L$, and free-end velocity, $(\partial w/\partial t)_L$, have opposite signs over most of the oscillation cycle. This dragging, lagging motion is actually observed during experiments once the critical flow velocity for flutter has been attained (Gregory and Païdoussis, 1966b). Thus, for $\Delta W > 0$, free motions of the system are amplified, i.e. the cantilevered pipe flutters.

Recalling that $\partial^2 w/\partial x^2 \approx 1/R$, where R is the local radius of curvature, it is obvious that the second term in Eq. (1) is a centrifugal term, while the third is a Coriolis term; as first shown by Benjamin (1961), flutter arises by the interaction of these two kinds of forces. However, the $MU^2(\partial^2 w/\partial x^2)$ term may also be viewed as a compressive force,[1] associated to the fluid momentum MU^2 emerging from the free end, always tangential to it – thus, a *follower* tangential compressive force. This mathematically obvious statement is physically counter-intuitive, as fluid friction actually stretches the pipe, something that is easily visible in experiments.[2] This matter will be elucidated later by the work to be presented.

Analytical solutions to Eq. (1) by a particular method developed by Gregory and Païdoussis (1966a) as well as by a Galerkin method support the conclusions arrived at above via energy considerations. Small flow velocities U induce damping in all modes of the system, increasing with U; however, at higher U the effect is reversed, and at sufficiently high U the system becomes unstable by flutter in its second mode via a Hopf bifurcation.

Many variants of the basic system modelled via Eq. (1) have been considered. For example, a vertical pipe conveying fluid was studied theoretically and experimentally (Païdoussis, 1970), such that gravity effects need to be taken into

[1] If the pipe were subjected to an external tension, $\overline{T}$, a term $-\overline{T}(\partial^2 w/\partial x^2)$ would have to be added to the equation of motion; but here we have something like $+\overline{T}(\partial^2 w/\partial x^2)$.

[2] It should be stressed that Eq. (1) was derived via a *viscous* plug-flow model. The fact that frictional terms do not appear explicitly in the equation of motion is simply the result of the traction on the pipe and pressure-drop-related forces in the fluid cancelling out exactly (Benjamin, 1961; Païdoussis, 1998).

account. The dynamical behaviour was found to be similar to that discussed in the foregoing. Bajaj and Sethna (1984) found that, in general, the flutter can be either planar or rotational (three-dimensional), depending on a parameter β, defined here in Eq. (6). Also, the case of a vertical cantilevered pipe with an end-mass [see Fig. 1(a)] was studied, mainly experimentally, by Copeland and Moon (1992), considering also nonlinear effects. It was found that, beyond the threshold of flutter, higher-order bifurcations arise, with intricate, generally three-dimensional patterns of motion, eventually leading to chaos. Further work on this problem was conducted, both theoretically and experimentally, by Païdoussis and Semler (1998) and Modarres-Sadeghi et al. (2007).

The system considered here is shown in Fig. 1. It is a vertical cantilevered pipe conveying fluid, fitted with an end-piece at the free end. As shown in Fig. 1(b), when the end-piece is unplugged, the fluid simply passes straight through;[3] alternatively, as shown in Fig. 1(c), when the end-piece is plugged, the flow emerges through the side-holes, perpendicular to the long axis of the pipe. The dynamics in these two flow configurations is studied both experimentally and theoretically.

2. Theoretical investigation

2.1. Theoretical model

The linear equation of motion for the system of Fig. 1 is as follows (Païdoussis and Issid, 1974; Semler and Païdoussis, 1995; Païdoussis and Semler, 1998; Païdoussis, 1998):

$$EI\left[1+\left(\overline{\alpha}+\frac{\overline{\mu}^*}{\Omega}\right)\frac{\partial}{\partial t}\right]\frac{\partial^4 w}{\partial x^4}+(MU^2-\overline{T})\frac{\partial^2 w}{\partial x^2}-\left\{\int_x^L [M+m+m_e\delta(x-L)]g\,\mathrm{d}x\right\}\frac{\partial^2 w}{\partial x^2}+2MU\frac{\partial^2 w}{\partial x\,\partial t}$$
$$+[M+m+m_e\delta(x-L)]g\frac{\partial w}{\partial x}+[M+m+m_e\delta(x-L)]\frac{\partial^2 w}{\partial t^2}=0, \tag{3}$$

where in addition to the parameters in Eq. (1), m_e is the mass of the end-piece, modelled as a point-mass, $\overline{T}$ is a mean tension applied to the pipe, g is the acceleration due to gravity, Ω is the oscillation frequency measured in rad/s, $\delta(x-L)$ is the Dirac delta function, and $\overline{\alpha}$ and $\overline{\mu}^*$ are constants in the *ad hoc* visco-hysteretic model developed to represent the dissipative forces in the elastomer pipes used in the experiments; specifically, $\overline{\mu}^*$ is the hysteretic damping coefficient and $\overline{\alpha}$ is the Kelvin–Voigt type viscoelastic damping coefficient (Païdoussis and Des Trois Maisons, 1971). Eq. (3) may be rendered dimensionless through the use of the following dimensionless parameters:

$$\xi=\frac{x}{L},\quad \eta=\frac{w}{L},\quad \tau=\left(\frac{EI}{M+m}\right)^{1/2}\frac{t}{L^2}, \tag{4}$$

to yield

$$\left[1+\left(\overline{\alpha}^*+\frac{\overline{\mu}^*}{\omega}\right)\frac{\partial}{\partial\tau}\right]\frac{\partial^4\eta}{\partial\xi^4}+(u^2-\Gamma)\frac{\partial^2\eta}{\partial\xi^2}-\gamma\left\{\int_\xi^1[1+\Gamma_e\delta(\xi-1)]\,\mathrm{d}\xi\right\}\frac{\partial^2\eta}{\partial\xi^2}+2\beta^{1/2}u\frac{\partial^2\eta}{\partial\xi\,\partial\tau}+\gamma[1+\Gamma_e\delta(\xi-1)]\frac{\partial\eta}{\partial\xi}$$
$$+[1+\Gamma_e\delta(\xi-1)]\frac{\partial^2\eta}{\partial\tau^2}=0, \tag{5}$$

where

$$u=\left(\frac{M}{EI}\right)^{1/2}UL,\quad \beta=\frac{M}{M+m},\quad \gamma=\frac{(M+m)gL^3}{EI},\quad \Gamma_e=\frac{m_e}{(m+M)L},$$
$$\Gamma=\frac{\overline{T}L^2}{EI},\quad \overline{\alpha}^*=\left(\frac{EI}{M+m}\right)^{1/2}\frac{\overline{\alpha}}{L^2},\quad \omega=\left(\frac{M+m}{EI}\right)^{1/2}\Omega L^2; \tag{6}$$

$\overline{\mu}^*$ is dimensionless *ab initio*.

The system is discretized following the Galerkin procedure, thereby assuming a solution of the form

$$\eta(\xi,\tau)=\sum_{r=1}^{N}\phi_r(\xi)q_r(\tau), \tag{7}$$

[3]Even though the side-holes are not blocked, the fluid is not diverted perpendicularly since resistance through the side-holes is much higher than that for straight-through flow.

where $\phi_r(\xi)$ are the comparison functions, taken here to be the cantilevered beam eigenfunctions, and $q_r(\tau)$ are the generalized coordinates. Eq. (7) is substituted into Eq. (5) to give

$$\sum_{r=1}^{N}\{\lambda_r^4\phi_r q_r + (\overline{\alpha}^* + \overline{\mu}^*/\omega)\lambda_r^4\phi_r\dot{q}_r + (u^2-\Gamma)\phi_r'' q_r - \gamma[(1-\xi)+\Gamma_e]\phi_r'' q_r + 2\beta^{1/2}u\phi_r'\dot{q}_r + \gamma[1+\Gamma_e\delta(\xi-1)]\phi_r' q_r + [1+\Gamma_e\delta(\xi-1)]\phi_r\ddot{q}_r\} = 0. \tag{8}$$

Thereafter, Eq. (8) is multiplied by $\phi_s(\xi)$ and integrated over the domain [0, 1], giving

$$\lambda_r^4\delta_{sr}q_r + (\overline{\alpha}^* + \overline{\mu}^*/\omega)\lambda_r^4\delta_{sr}\dot{q}_r + (u^2-\Gamma)c_{sr}q_r - \gamma(1+\Gamma_e)c_{sr}q_r + \gamma d_{sr}q_r + 2\beta^{1/2}ub_{sr}\dot{q}_r + \gamma b_{sr}q_r + \gamma\Gamma_e\phi_s(1)\phi_r'(1)q_r + \delta_{sr}\ddot{q}_r + \Gamma_e\phi_s(1)\phi_r(1)\ddot{q}_r = 0, \tag{9}$$

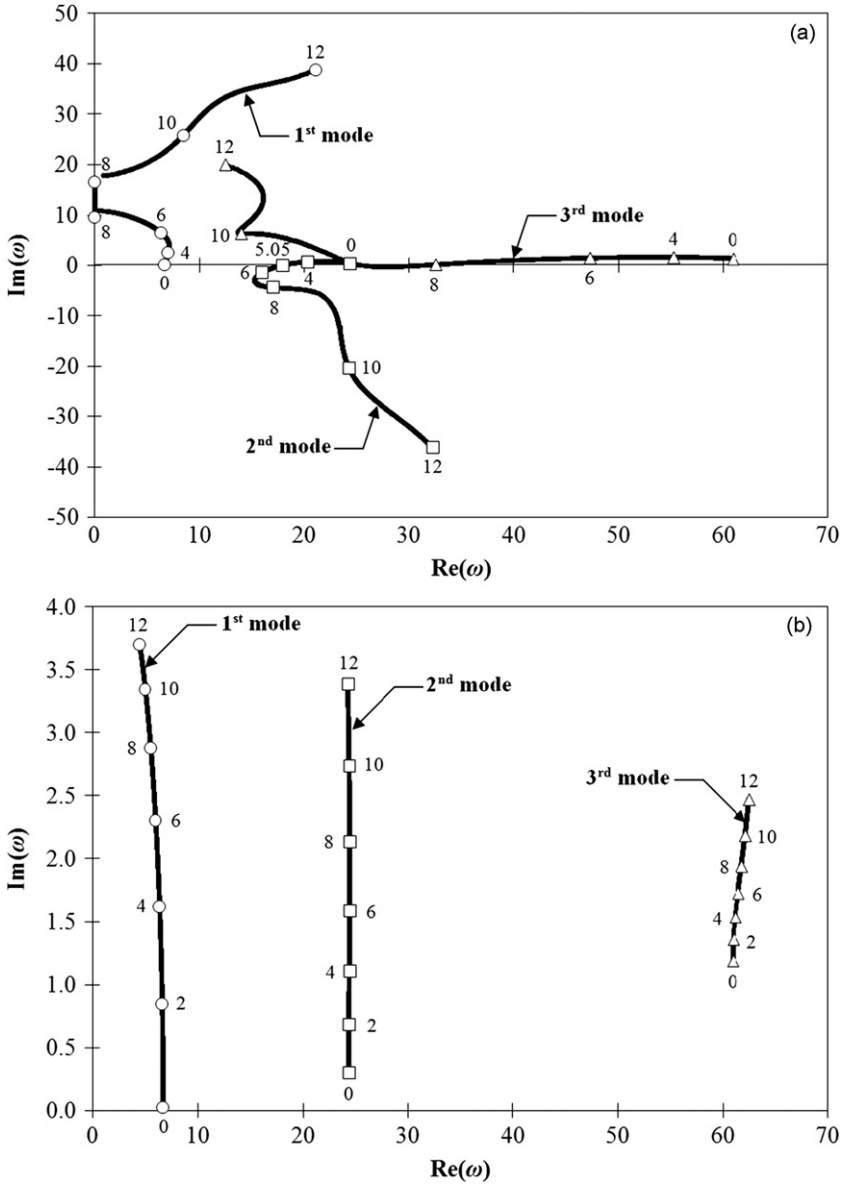

Fig. 2. Argand diagram ω as a function of u for a flexible cantilevered pipe with $\beta = 0.142$, $\gamma = 27.6$, $\Gamma_e = 0.196$, $\overline{\alpha}^* = 0.00017$, and $\overline{\mu}^* = 0.03927$, obtained using a five-mode Galerkin approximation, for (a) straight-through flow and (b) 90° diverted-flow.

where

$$\delta_{sr}=\int_0^1 \phi_s\phi_r\,\mathrm{d}\xi,\quad b_{sr}=\int_0^1 \phi_s\phi_r'\mathrm{d}\xi,\quad c_{sr}=\int_0^1 \phi_s\phi_r''\,\mathrm{d}\xi,\quad d_{sr}=\int_0^1 \phi_s\phi_r''\xi\,\mathrm{d}\xi; \tag{10}$$

expressions for these integrals are available [see Païdoussis (1998, p. 87)]. Eq. (9) may be written in the compact form

$$[M]\ddot{\mathbf{q}}+[C]\dot{\mathbf{q}}+[K]\mathbf{q}=\mathbf{0}, \tag{11}$$

where $\boldsymbol{q}=\{q_1, q_2, q_3,\ldots,q_N\}^{\mathrm{T}}$. The elements of the mass, $[M]$, damping, $[C]$, and stiffness, $[K]$, matrices in Eq. (11) are determined from Eq. (9) to be

$$\begin{aligned} &M_{sr}=\delta_{sr}+\Gamma_e\phi_s(1)\phi_r(1),\quad C_{sr}=(\overline{\alpha}^*+\overline{\mu}^*/\omega)\lambda_r^4\delta_{sr}+2\beta^{1/2}ub_{sr},\\ &K_{sr}=\lambda_r^4\delta_{sr}+\gamma b_{sr}+[u^2-\Gamma-\gamma(1+\Gamma_e)]c_{sr}+\gamma d_{sr}+\gamma\Gamma_e\phi_s(1)\phi_r'(1). \end{aligned} \tag{12}$$

2.2. Theoretical results

The system studied in this section is a flexible cantilevered pipe with $\beta=0.142$, $\gamma=27.6$, $\Gamma_e=0.196$, $\overline{\alpha}^*=0.00017$, and $\overline{\mu}^*=0.03927$.

Fig. 2(a) presents the Argand diagram, obtained using a five-mode Galerkin approximation, for the three lowest modes of the system as a function of the dimensionless flow velocity, u, for the unblocked pipe fitted with a four-holed end-piece. It should be mentioned that the horizontal axis is the real component of the dimensionless complex frequency, $\mathrm{Re}(\omega)$, which represents the oscillation frequency of the system, while the vertical axis is the imaginary component of the dimensionless complex frequency, $\mathrm{Im}(\omega)$, which is related to the damping of the system; specifically, the damping ratio is $\zeta=\mathrm{Im}(\omega)/\mathrm{Re}(\omega)$. Thus, positive values of $\mathrm{Im}(\omega)$ give rise to damped oscillations, while negative values of $\mathrm{Im}(\omega)$ result in amplified oscillations. Fig. 2(a) illustrates that the system loses stability by second-mode flutter at a critical flow velocity of $u_1=5.05$ and with a critical oscillation frequency of $\mathrm{Re}(\omega_1)=17.9$.

Fig. 2(b) presents the Argand diagram, again obtained using a five-mode Galerkin approximation, for the first three modes of the blocked pipe as a function of the dimensionless flow velocity, u. In this case, the flow emerges from the four side-holes of the end-piece. As the straight-through flow is blocked, a tensile force is generated at the end, and hence throughout the pipe, equal to $\overline{T}=MU^2$; hence, $\Gamma=u^2$. As seen in Fig. 2(b), the flow induces damping in all three modes, increasing with u. There is no reversal of this trend up to $u=12$ and, from the evidence of this figure, none seems likely.

The mechanism for the disappearance of flutter in this case becomes obvious by considering the simplified form of Eq. (3), with dissipative and gravity effects neglected:

$$EI\frac{\partial^4 w}{\partial x^4}+(MU^2-\overline{T})\frac{\partial^2 w}{\partial x^2}+2MU\frac{\partial^2 w}{\partial x\partial t}+[M+m+m_e\delta(x-L)]\frac{\partial^2 w}{\partial t^2}=0. \tag{13}$$

It is clear that, with the straight-through flow blocked, and $\overline{T}=MU^2$, the compressive-centrifugal second term in the equation vanishes. The only remaining effect of the flow on the pipe is associated with Coriolis forces, which (as in the freely discharging case) introduce flow-induced damping, ever increasing with increasing flow, as in Fig. 2(b).

3. Experimental investigation

3.1. Experimental apparatus

The experiments were performed with a flexible elastomer pipe and a plastic end-piece with four side-holes azimuthally at 90° from each other. The fluid conveyed was water. The pipes were cast using a two-part silicone rubber kit consisting of a base and a curing agent. It should be mentioned that a small elastomer ring was embedded at one end of the pipe during the casting process in order to facilitate mounting the end-piece onto the pipe during experiments. Furthermore, the end-piece was designed with a removable plug. Thus, the plugged end-piece allowed for a 90° diversion of the flow at the downstream end of the cantilevered pipe, while an unplugged end-piece allowed the straight-through passage of the flow (see Fig. 1).

The geometrical and physical properties of the pipe and end-piece are summarized in Table 1. Note that f_n and δ_n are the natural frequency and log decrement of the pipe in the nth mode. For higher modes, i.e. $n\geq 4$, the log decrement of

the system (needed in the theoretical model) was approximated by $\delta_n = 0.0516n - 0.0144$, which is the linear regression line that best fits the experimental data for the first three modes.

The experimental apparatus is shown in Fig. 3. It consists mainly of (i) a cantilevered pipe vertically hung, over (ii) a collecting tank, which rests on weighing scales, (iii) a centrifugal pump, which supplies recirculating water from a reservoir rather than from the mains, (iv) an Omega FMG710 magnetic flowmeter, which measures the volumetric flow rate, and (v) an Optron system, which is a non-contact electro-optical biaxial displacement follower system that consists of an optical head and a control unit. The combination of a flow straightener and an accumulator tank, which attenuates pulsations from the centrifugal pump, ensures that the flow is uniform at the inlet of the pipe. The Optron system is used, together with the LabVIEW graphical programming software, to acquire a time signal of the motion of the pipe at a point along its length. The acquired time signals are then analyzed using MATLAB to determine the oscillation frequencies of the pipe at various flow velocities. Additional information regarding the experimental apparatus may be found in Païdoussis and Semler (1998).

3.2. Experimental results

The dynamical behaviour of the unblocked system is as follows. At low flow velocities, the system experienced an increase in damping with increasing internal flow, as could be seen by slightly perturbing the pipe. As the flow velocity

Table 1
The geometrical and physical properties of the pipe and end-piece.

D_o (m)	D_i (m)	L (m)	EI (N m^2)	m (kg/m)	M (kg/m)	β (Dimen.)	γ (Dimen.)	m_e (kg)
0.0159	0.00635	0.448	7.11×10^{-3}	0.191	0.0317	0.142	27.6	0.0195
Γ_e (Dimen.)	$\overline{\alpha}^*$ (Dimen.)	$\overline{\mu}^*$ (Dimen.)	f_1 (Hz)	f_2 (Hz)	f_3 (Hz)	δ_1 (Dimen.)	δ_2 (Dimen.)	δ_3 (Dimen.)
0.196	0.00017	0.03927	1.07	4.10	10.2	0.0346	0.0937	0.138

Dimen. = dimensionless.

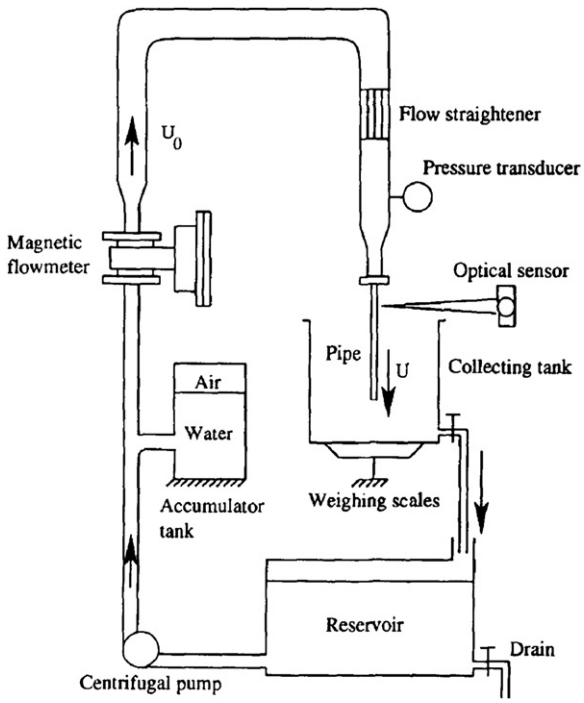

Fig. 3. Schematic of the experimental apparatus (Païdoussis and Semler, 1998).

Table 2
The theoretical and experimental critical flow velocities and oscillation frequencies for the straight-through flow configuration, where the multiplicative factor to switch from u_{cr} to U_{cr} in m/s is 1.06 and that to switch from $\mathrm{Re}(\omega_{cr})$ to f_{cr} in Hz is 0.142.

	Theory	Experiment
u_{cr}	5.05	5.46
$\mathrm{Re}(\omega_{cr})$	17.9	16.3

was increased further, the pipe experienced a decrease in damping, which eventually became negative via a Hopf bifurcation. This gave rise to limit-cycle motion, involving two-dimensional, planar, second beam-mode flutter, with a strong travelling-wave component. As the flow was increased further, a second bifurcation was encountered, characterized by two-dimensional, planar, fixed-node type flutter involving third beam-mode shape oscillations, and a fixed node at approximately mid-length, and with a higher oscillation frequency. At even higher flows, the oscillation frequency increased further, and more complex vibrational modes were observed. Eventually, the motion became chaotic, and impacting occurred with the walls of the collecting tank; at this point, the experiment was discontinued. It was remarked that the cantilevered pipe exhibited three-dimensional, transient behaviour just prior to the onset of the first and second bifurcations for only brief periods of time; during this time, the system searched for and located its preferred two-dimensional plane of motion for the planar limit-cycle flutter. The reader is referred to Electronic Annex 1 for a video clip showing the dynamics of the unblocked pipe.

In contrast, the dynamical behaviour of a cantilevered pipe with a plugged end-piece was entirely different. For this system, the pipe did not display any oscillatory motion, or any other instability for that matter, as predicted. Indeed, the system remained stable over the full flow range attainable. Experiments with an end-piece with eight side-holes azimuthally at 45° to each other yielded sensibly the same results. The reader is referred to Electronic Annex 2 for a video clip showing the dynamics of the blocked pipe.

4. Comparison of experiment to theory and nonlinear behaviour

The experimental threshold for flutter of the cantilevered pipe fitted with an unplugged end-piece is compared with prediction of linear theory obtained by solving Eq. (5). However, as discussed in Section 3.2, there is a rich experimental post-flutter dynamical behaviour; this was explored by means of the nonlinear theoretical model of Wadham-Gagnon et al. (2007); see also Modarres-Sadeghi et al. (2007).

The theoretical and experimental flutter threshold values of the dimensionless critical flow velocity, u_{cr}, and the dimensionless critical oscillation frequency, $\mathrm{Re}(\omega_{cr})$, are compared in Table 2. Moreover, a bifurcation diagram obtained by the nonlinear theory with six Galerkin modes is given in Fig. 4,[4] showing the evolution of the dimensionless free-end displacement, $\eta(1)$, with the dimensionless flow velocity, u, for system parameters corresponding to those of the experimental system.

From Fig. 4, it is seen that the system is stable for $u<u_1=5.0$, and loses stability by travelling-wave type flutter at $u_1\approx 5.0$. Fixed-node type flutter of smaller amplitude then develops at $u_2\approx 6.8$, and the motion of the system becomes more complex for $u_3>9.0$. The corresponding experimental values are $u_1=5.46$ and $u_2=8.53$, where u_1 is in reasonably good agreement with theory, but not u_2. The reason for this latter is most probably that the rotational inertia of the end-mass was not taken into account in the theoretical model. As the post-flutter nonlinear characteristics of the system were not the primary purpose of this Communication, the matter was not pursued further.

In the case of the blocked straight-through path, there is no bifurcation at all, the system remaining stable at its equilibrium state. Thus, nonlinear analysis here would be meaningless.

5. Conclusion

The dynamics of a flexible cantilevered pipe discharging water and fitted with a special end-piece has been investigated, both theoretically and experimentally. The end-piece may be used (i) in its ''unblocked'' configuration, allowing fluid to be discharged freely, straight through; or (ii) in the ''blocked'' mode, in which case the flow exits via

[4]The first two bifurcations with four Galerkin modes occur at the same u.

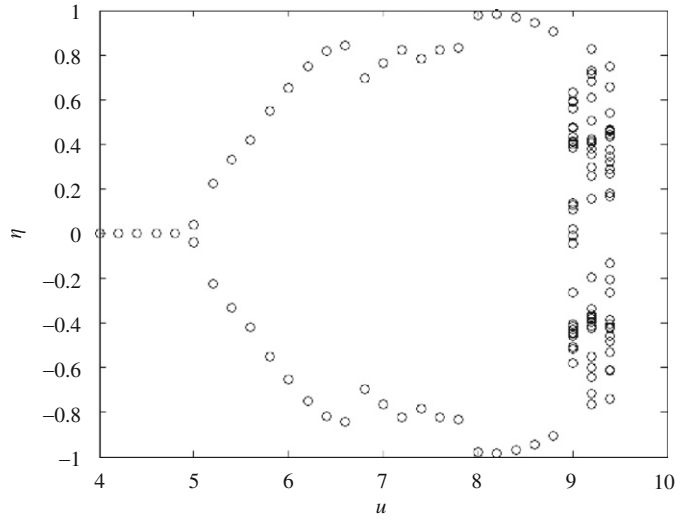

Fig. 4. Bifurcation diagram for a flexible cantilevered pipe with $\beta = 0.142$, $\gamma = 27.6$, $\Gamma_e = 0.196$, $\overline{\alpha}^* = 0.00017$, and $\overline{\mu}^* = 0.03927$ using $N = 6$ modes for the straight-through flow configuration.

side-holes, perpendicular to the pipe axis. In case (i), the system loses stability by flutter at high enough flow velocity, and then develops more complex oscillatory patterns at higher flow. In case (ii), the system remains inert and stable over the full range of attainable flow velocities.

It is shown that the absence of flutter in case (ii) is related to the generation of a tensile force by the blocked straight-through flow-path, which exactly cancels the centrifugal-compressive force which is essential in the generation of flutter. Thus, the compression due to the exiting jet becomes physically easy to grasp. In this regard, the plugged end-piece may be viewed as an effective stabilizing device.

The post-flutter nonlinear behaviour of the system in case (i) is compared with nonlinear theory and is found to be in qualitatively good agreement with the observed behaviour (though not so good quantitatively).

A more detailed account of the theory and the experimental work may be found in Rinaldi (2009).

Acknowledgements

The authors gratefully acknowledge the financial support by the Natural Sciences and Engineering Research Council of Canada (NSERC) and le Fonds Québécois de la Recherche sur la Nature et les Technologies (FQRNT). The authors are also grateful to Dr C. Semler, Dr Y. Modarres-Sadeghi and Mr M. Hajghayesh for making available the nonlinear code that was used in the calculations of Section 4.

Appendix A. Supplemental material

Supplementary data associated with this article can be found in the online version at doi:10.1016/j.jfluidstructs.2010.01.004.

References

Bajaj, A.K., Sethna, P.R., 1984. Flow induced bifurcations to three-dimensional oscillatory motions in continuous tubes. SIAM Journal on Applied Mathematics 44, 270–286.

Benjamin, T.B., 1961. Dynamics of a system of articulated pipes conveying fluid. I. Theory. Proceedings of the Royal Society of London, Series A261, 457–486.

Copeland, G.S., Moon, F.C., 1992. Chaotic flow-induced vibration of a flexible tube with end mass. Journal of Fluids and Structures 6, 705–718.

Gregory, R.W., Païdoussis, M.P., 1966a. Unstable oscillation of tubular cantilevers conveying fluid. I. Theory. Proceedings of the Royal Society of London, Series A293, 512–527.

Gregory, R.W., Païdoussis, M.P., 1966b. Unstable oscillation of tubular cantilevers conveying fluid. II. Experiments. Proceedings of the Royal Society of London, Series A293, 528–542.

Modarres-Sadeghi, Y., Semler, C., Wadham-Gagnon, M., Païdoussis, M.P., 2007. Dynamics of cantilevered pipes conveying fluid. Part 3: Three-dimensional dynamics in the presence of an end-mass. Journal of Fluids and Structures 23, 589–603.

Païdoussis, M.P., 1970. Dynamics of tubular cantilevers conveying fluid. Journal of Mechanical Engineering Science 12, 85–103.

Païdoussis, M.P., 1998. Fluid–Structure Interactions: Slender Structures and Axial Flow, vol. 1. Academic Press Limited, London.

Païdoussis, M.P., Des Trois Maisons, P.E., 1971. Free vibration of a heavy, damped, vertical cantilever. Journal of Applied Mechanics 38, 524–526.

Païdoussis, M.P., Issid, N.T., 1974. Dynamic stability of pipes conveying fluid. Journal of Sound and Vibration 33, 267–294.

Païdoussis, M.P., Semler, C., 1998. Non-linear dynamics of a fluid-conveying cantilevered pipe with a small mass attached at the free end. International Journal of Non-Linear Mechanics 33, 15–32.

Rinaldi, S., 2009. Experiments on the dynamics of cantilevered pipes subjected to internal and/or external axial flow. M.Eng. Thesis, McGill University, Montreal.

Semler, C., Païdoussis, M.P., 1995. Intermittency route to chaos of a cantilevered pipe conveying fluid with a mass defect at the free end. Journal of Applied Mechanics 62, 903–907.

Wadham-Gagnon, M., Païdoussis, M.P., Semler, C., 2007. Dynamics of cantilevered pipes conveying fluid. Part 1: Nonlinear equations of three-dimensional motion. Journal of Fluids and Structures 23, 545–567.